RESEARCH PAPER

RNA Biology 12:6, 658–673; June 2015; Published with license by Taylor & Francis Group, LLC

The C-terminal region of the RNA helicase CshA is required for the interaction with the degradosome and turnover of bulk RNA in the opportunistic pathogen *Staphylococcus aureus*

Caroline Giraud[†], Stéphane Hausmann, Sylvain Lemeille, Julien Prados, Peter Redder, and Patrick Linder*

Department of Microbiology and Molecular Medicine; Medical Faculty; University of Geneva; Michel Servet, Geneva, Switzerland

[†]Present address: U2RM: Unité de Recherche Risques Microbiens; Université de Caen Basse-Normandie; Caen, France

Keywords: CshA, DEAD-box family, degradosome, RNA decay, RNase

Staphylococcus aureus is a versatile opportunistic pathogen that adapts readily to a variety of different growth conditions. This adaptation requires a rapid regulation of gene expression including the control of mRNA abundance. The CshA DEAD-box RNA helicase was previously shown to be required for efficient turnover of the *agr* quorum sensing mRNA. Here we show by transcriptome-wide RNA sequencing and microarray analyses that CshA is required for the degradation of bulk mRNA. Moreover a subset of mRNAs is significantly stabilised in absence of CshA. Deletion of the C-terminal extension affects RNA turnover similar to the full deletion of the *cshA* gene. In accordance with RNA decay data, the C-terminal region of CshA is required for an RNA-independent interaction with components of the RNA degradation machinery. The C-terminal truncation of CshA reduces its ATPase activity and this reduction cannot be compensated at high RNA concentrations. Finally, the deletion of the C-terminal extension does affect growth at low temperatures, but to a significantly lesser degree than the full deletion, indicating that the core of the helicase can assume a partial function and opening the possibility that CshA is involved in different cellular processes.

Introduction

Staphylococcus aureus is a Gram-positive opportunistic pathogen that colonizes 20–50% of human population.[1] Depending on its growth phase and bacterial density, it expresses various virulence factors, including exotoxins and haemolysins, which lead to a large spectrum of diseases, from benign skin infection to severe osteomyelitis, endocarditis, and sepsis.[2,3] In addition to the fact that *S. aureus* possesses the entire molecular arsenal to develop infections, it can also be resistant against various antibiotics, raising major public health issues.[4] Moreover, *S. aureus* is able to survive and adapt to many environmental conditions, such as biofilm formation or intracellular growth, contributing to the persistence of *S. aureus* infections and rendering eradication of this pathogen difficult, even with harsh treatments.[5] The adaptation to different growth and stress conditions requires a tight regulation of gene expression, a dynamic process that is controlled at several levels of the flow of genetic information from DNA to proteins. Part of this regulation is obtained by regulating steady-state transcript levels that result from both RNA synthesis and degradation, i.e., RNA stability.

RNA helicases of the DEAD-box family play various but important roles in RNA metabolism.[6] All the DEAD box RNA helicases contain 12 conserved motifs gathered together in 2 RecA-fold domains that are involved in interactions with the RNA substrate and ATP. In addition to these 2 domains, composing the core of DEAD box helicases, they can possess N- or C-terminal extensions that can drive specific interactions with RNA[7] or regulatory proteins.[8,9] DEAD box RNA helicases function by coupling ATP binding and hydrolysis to changes in affinity for RNA. Many DEAD-box proteins use this basic mechanism for a mode of RNA helicase activity, separating the strands of short RNA duplexes in a process that involves no translocation. They can also function as ATP-dependent RNA clamps to provide nucleation-centers that allow binding of larger protein complexes to an RNA substrate. In prokaryotes, they are involved in ribosome biogenesis, RNA decay and translation initiation. This places the helicases as important regulators in gene expression.[10]

*Correspondence to: Patrick Linder; Email: patrick.linder@unige.ch
Submitted: 01/05/2015; Revised: 03/23/2015; Accepted: 03/24/2015
http://dx.doi.org/10.1080/15476286.2015.1035505

In *E. coli*, the DEAD box helicase RhlB is associated with the degradosome, a protein complex responsible for RNA degradation.[11,12] The RNase E endonuclease consists of a N-terminal domain that possess the catalytic activity and a C-terminal domain that serves as scaffold for the other degradosome proteins. In addition to RhlB, a 3′->5′ exonuclease polynucleotide phosphorylase (PNPase) and the glycolytic enzyme enolase, whose role in the complex is not understood, are part of the core complex. Other minor components, such as RraA, RraB,[13] Hfq,[14] L4,[15] polyphosphate kinase (PPK), DnaK, and GroEL, were also found to be associated with the degradosome.[16,17] Moreover, it has been shown that the *E. coli* degradosome associates with translating ribosomes.[18] During the mRNA degradation process, RNase E cleaves 5′ monophosphorylated RNAs that are subsequently degraded by the PNPase and other 3′->5′ exoribonucleases that are not associated with the degradosome (for review see ref. 19. RNase E and the PNPase are single-strand specific enzymes and RhlB activity is required to facilitate the RNA degradation in a context where the RNAs can form double-stranded structures.[20,21] Moreover, it has been shown that a C-terminal region of RNase E stimulates the RNA-dependent ATPase activity of RhlB.[22]

Bacterial two hybrid analyses have shown that the DEAD box helicase CshA of *S. aureus* is also part of a putative degradosome,[23] similar to its *Bacillus subtilis* counterpart.[24] The interaction network includes the endonuclease RNase Y, the endo and 5′->3′ exoribonucleases RNase J1 and RNase J2 and the 3′->5′ exonuclease PNPase. The complex also contains the RNaseP component RnpA, the glycolytic enzymes enolase and phosphofructokinase. Nevertheless, a complex containing several of these proteins has not yet been purified as such. Mutations in *cshA* revealed in addition to a cold sensitive phenotype a reduced biofilm formation and increased hemolysis, the latter due to a stabilization of *agr* mRNA.[25] In this context, CshA could be needed to allow the degradosome enzymes to degrade the RNA, as it was shown for RhlB. In *H. pylori* it has been shown that, *in vitro*, the DEAD box RNA helicase RhpA allows RNase J to degrade double-stranded RNA.[26] The ribonucleases RNase Y, RNase J1, RNase J2 and PNPase are specific for single-stranded RNA and a stable duplex on the RNA can form a protective structure to prevent degradation.[27] The unwinding of such structures by CshA would allow the degradosome to degrade this RNA.

In this work we show that the C-terminal domain of CshA is necessary for its function *in vivo*, confirming the importance of the DEAD box accessory domains. We show that CshA is implicated in the control of the stability of several mRNAs, including many that encode regulators or virulence factors. Finally we show that CshA interacts *in vivo* with degradosome components and that the C-terminal domain of CshA is important for these interactions.

Results

The C-terminal region of CshA plays a crucial role

DEAD-box proteins contain 2 domains with a RecA fold, constituting together the core or motor domain involved in ATP dependent RNA binding and RNA-dependent ATP hydrolysis. Accessory N- or C-terminal extensions of the DEAD box helicases can play a regulatory or/and a specificity role. We therefore investigated whether the C-terminal extension of CshA is required for its function and deleted the region corresponding to amino acids 383 to 506, creating a protein similar in length to eIF4A, the godfather of DEAD-box proteins[28] (**Fig. 1A, Fig. S1**). The region after amino acid 434 appears to be unstructured by contrast to the globular catalytic core of the protein (GlobPlot 2.3,[29]). To avoid changes in the expression level, we deleted the corresponding region of the gene directly on the chromosome using the *pyrEF*/5-FOA selection/antiselection system[30] in a derivative of the clinical strain SA564,[31] resulting in strain PR01*cshA*ΔCter. We checked by western blot that the truncated protein was still correctly expressed (**Fig. 1B**). To assess the function of the truncated protein, we followed 2 readouts for CshA activity, the cold sensitive phenotype and the *agr* mRNA decay. The PR01*cshA*ΔCter strain showed a cold sensitive phenotype at 16°C similar to the full deletion of the *cshA* gene. Interestingly, at 24°C only the PR01Δ*cshA* strain showed a cold sensitivity phenotype whereas the PR01*cshA*ΔCter strain was still able to grow. Importantly, growth at 16°C can be restored in PR01*cshA*ΔCter by expressing CshA from a plasmid. At 42°C, 37°C and 30°C both strains have a growth similar to the parental PR01 strain (**Fig. 1C**). Since we have previously shown that a *cshA* mutant strain is affected in the decay of the *agr* quorum sensing mRNA, we also measured the decay of this mRNA in the PR01*cshA*ΔCter strain by qRT-PCR. A time course after rifampicin treatment showed that the *agr* mRNA decay was comparable to the PR01Δ*cshA* strain, showing that the C-terminal extension of CshA is of great importance *in vivo* for the RNA turnover function of the protein (**Fig. 1D**).

The truncated version of CshA retains ATPase activity

The reduced *in vivo* functionality of the C-terminal truncated RNA helicase could be due to lack of interactions with partner proteins or simply be due to the absence of enzymatic activity. We therefore expressed and purified the full length and the truncated proteins from *E. coli* and checked for their ATPase activity *in vitro* in presence or absence of rRNA.

Purification of the CshA-His protein was achieved by adsorption to nickel-agarose and elution with 250 mM imidazole. The nickel-agarose preparation was highly enriched with respect to the CshA-His polypeptide, as judged by SDS-PAGE (**Fig. 2A**). In parallel we purified a mutated version of CshA in which Lys52 in motif I (Walker A motif) was replaced by alanine (K52A; **Fig. 2A**). An analogous mutation in eIF4A was shown to abrogate nucleotide binding.[32] Recombinant wild-type CshA catalyzed the release of Pi from [gamma-^{32}P]ATP in the presence of *E. coli* rRNA (rRNA) and the extent of ATP hydrolysis was proportional to enzyme concentration (**Fig. 2B**). The ATPase activity of the K52A mutant was < 1% of the activity of wild-type enzyme. We therefore conclude that the observed phosphohydrolase activity is intrinsic to CshA. Moreover, the ATPase activity measured after a glycerol gradient followed exactly the position of the protein as determined by Western analysis (see below). As it was reported previously and characteristic for most DEAD-box

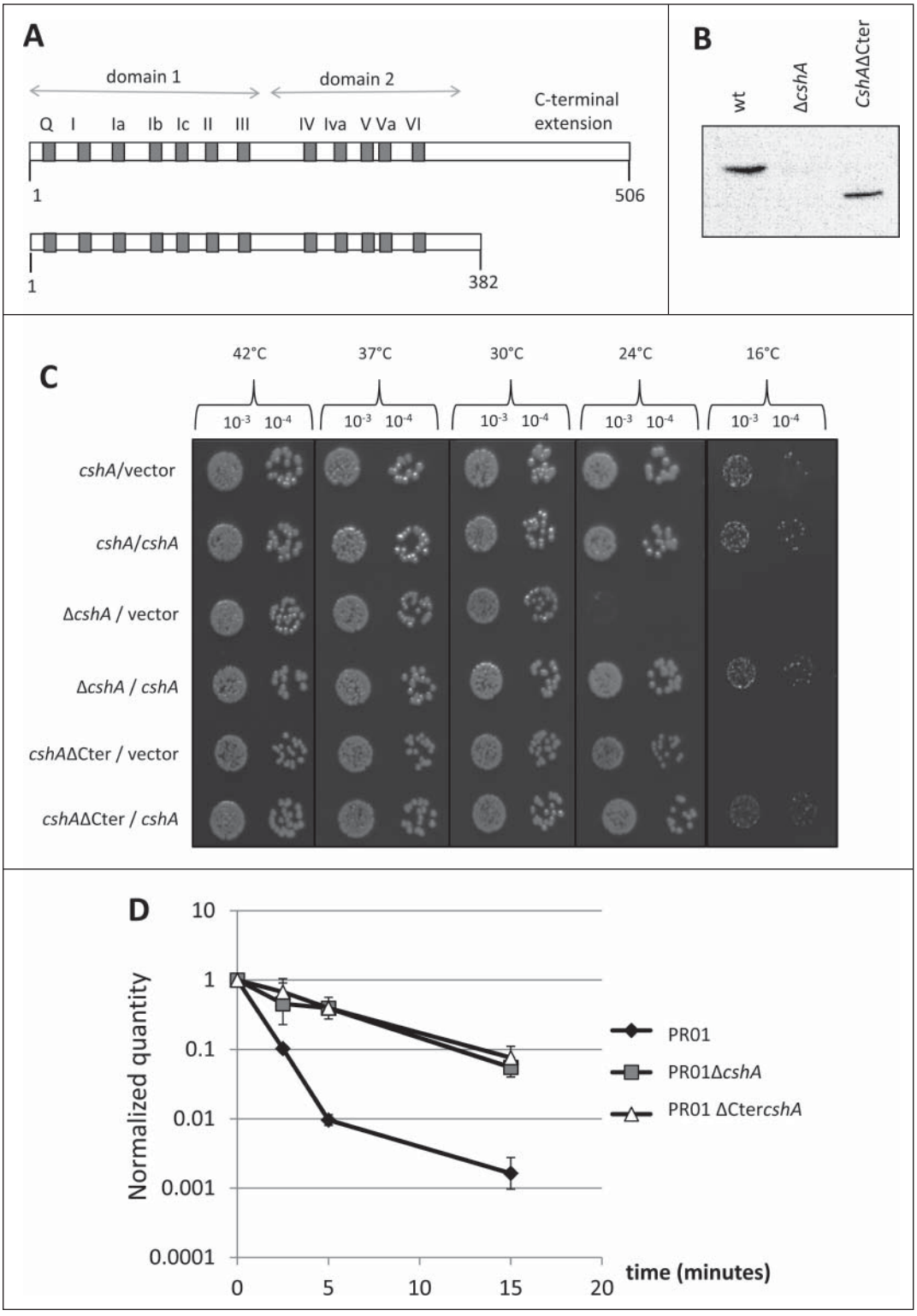

Figure 1. Functional analysis of CshA and CshAΔCter. (**A**) Schematic representation of the CshA protein. Gray boxes and the letters above represent the conserved domains characteristic of the DEAD-box family. The numbers below indicate the amino acid position. For CshAΔCter, the protein was truncated after amino acid 382. (**B**) Presence of CshA in the total cell extracts of PR01, PR01Δ*cshA* and PR01*cshA*ΔCter. The CshA protein was detected in a western blot performed with an anti-CshA polyclonal antibody. Equal amounts of lysed cells were loaded and verified by Ponceau staining. (**C**) The strains PR01, PR01Δ*cshA* and PR01*cshA*ΔCter, containing the plasmids pEB01 (vector) or pEB07 (containing CshA) were spotted in serial dilutions (indicated above) on rich medium containing 15 μg/ml chloramphenicol. All plates were incubated at 42°C (24 h), 37°C (24 h), 30°C (48 h), 24°C (3 days) and 16°C (6 days). Only representative 10^{-3} and 10^{-4} dilutions are shown. (**D**) Cultures of PR01 (black diamonds), PR01Δ*cshA* (gray squares) and the PR01*cshA*ΔCter (white triangles) were rifampicin treated to block *de novo* RNA synthesis. Samples were taken for RNA isolation at 0, 2.5, 5, 10 and 15 min after treatment, and qRT-PCR was performed using primers and probes specific for *agrA*, and using *HU* mRNA as an internal reference. The quantity of *agr*, relative to *HU*, was normalized to 1 at time zero, and plotted in the graph. Error bars represent the 99% confidence level.

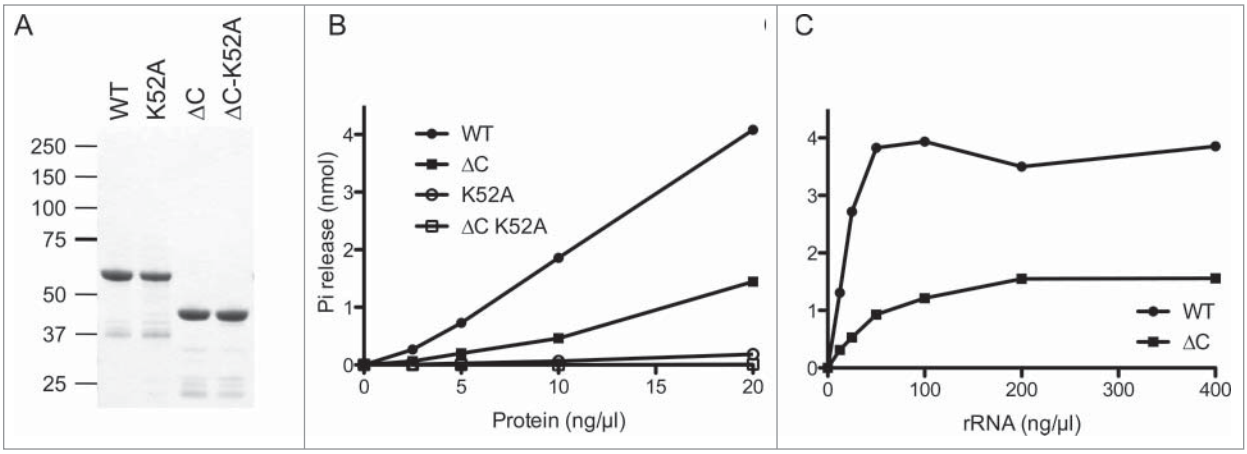

Figure 2. ATPase activity of the full length and the truncated CshA proteins. (**A**) CshA purification. Aliquots (3 μg) of the nickel-agarose preparations of wild-type (WT) CshA, mutant K52A, deletion mutant CshA△Cter, and deletion mutant CshA△CTer-K52A were analyzed by electrophoresis through a denaturing 4–12% Bis-Tris polyacrylamide gel. The polypeptides were visualized by staining with Commassie Blue dye. The positions and sizes (in kDa) of marker proteins are indicated on the left. (**B**) ATPase reaction mixtures (15 μl) containing 50 mM Tris-HCl, pH 8.0, 1 mM DTT, 2 mM $MgCl_2$, 1 mM [γ-^{32}P]ATP, 0.2 ng/μl rRNA and wild-type (WT) CshA or mutants CshA as specified were incubated at 37°C for 15 min. The extents of ATP hydrolysis are plotted as a function of input protein. (**C**) ATPase reaction mixtures (15 μl) containing 50 mM Tris-HCl, pH 8.0, 1 mM DTT, 2 mM $MgCl_2$, 1 mM [γ -^{32}P] ATP, either 20 ng wild-type (WT) CshA or 20 ng deletion mutant CshA△Cter, and an increasing amounts of rRNA as specified were incubated at 37°C for 15 min. The extents of ATP hydrolysis are plotted as a function of input rRNA.

proteins, only background ATPase activity could be detected in absence of RNA (data not shown).

The truncated CshA△Cter and its K52A version were also expressed in *E. coli* and purified in parallel. The mobility of the CshA△Cter proteins during SDS-PAGE was fairly consistent with their calculated sizes of 43 kDa (**Fig. 2A**). At saturating RNA concentrations, the CshA△Cter (1–382) protein retained 30% specific activity of wild type whereas the CshA△Cter-K52A was <1 % of the wild-type enzyme. We concluded that the C-terminal 124 amino acids of CshA are involved in, but not essential for, RNA dependent ATP hydrolysis (**Fig. 2B**).

To test the possible effects of the C-terminal domain deletion on the rRNA interactions of CshA, we measured ATP hydrolysis as a function of the concentration of the rRNA (**Fig. 2C**). Wild-type CshA and CshA△Cter displayed a typical hyperbolic dependence of ATP hydrolysis on input rRNA (**Fig. 2B**). From the titration curve we estimate that the deletion of the C-terminal domain elicited about a 3-fold decrement in the activation of the CshA ATPase. From this experiment we concluded that the C-terminal domain of CshA is not the major RNA interaction domain.

Sedimentation Analysis of CshA

The recombinant protein was subjected to zonal velocity sedimentation in a 15–30% glycerol gradient. Marker proteins catalase (native size 248 kDa), bovine serum albumin (66 kDa), and cytochrome c (12 kDa) were included as internal standards. CshA-His_6 (calculated to be a 57-kDa polypeptide) sedimented as a discrete peak (fraction 16) just slightly heavier than the BSA peak (66-kDa) (data not shown). The ATPase activity profile paralleled the abundance of the CshA-His_6 polypeptide and peaked at fraction 16 (**Fig. 3**). A plot of the S values of the 3 standards versus fraction number yielded a straight line (not shown). Interpolation to the internal standard curve determined an S value of 5.6 for CshA-His by suggesting that CshA-His is a homodimer in solution.

CshA is required for the decay of a subset of mRNAs in *S. aureus*

CshA was suggested to be part of the Firmicute degradosome,[23,24] and we have shown that CshA is involved in *agr* mRNA decay.[25] We therefore tested if the decay of other RNAs was also affected in absence of CshA or in absence of the C-terminal extension of CshA. The mutant and parental strains were grown to early exponential growth phase and transcription was stopped by the addition of rifampicin. Total bacterial RNA was purified from aliquots of cells before transcriptional arrest and at 2.5, 5, and 10 minutes post-transcriptional arrest. After depletion of rRNA, the purified RNA was then analyzed by RNA deep sequencing and the analysis of genes was fitted with the highly similar genome of N315. Genes that showed less than 100 reads on average over the 4 time points were eliminated, resulting in 1961 ORFs and tRNAs from strain SA564 out of the 2662 found in the N315 genome. The read counts were then normalized to the mRNA of HU, which was previously shown to be well expressed and relatively stable.[33] Similar to published studies,[34] these results clearly showed that most RNAs are present at background levels at >10 minutes after rifampicin treatment. Half-lives were computed by fitting a linear model on $\log_2$ transformed gene expressions. Genes whose RNA levels had the largest divergence with the fitted model are excluded to finally retain 1448 genes. Comparing the half-lives of each strain in the 2 experiments showed a good correlation of the 2 independent experiments (**Fig. S2**).

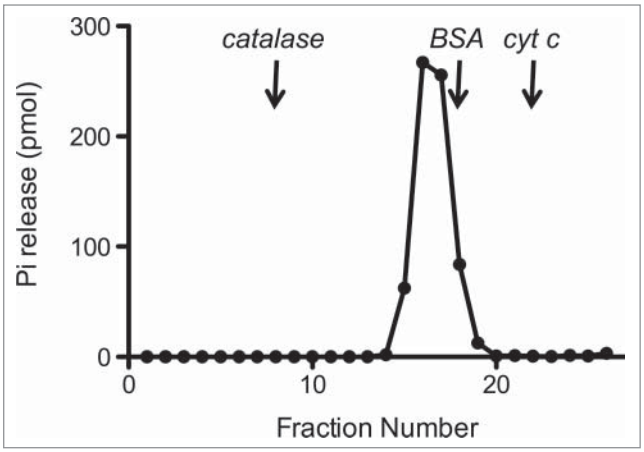

Figure 3. Sedimentation analysis of CshA.Recombinant CshA was sedimented in a glycerol gradient as described under "Materials and Methods." Aliquots (2 μl) of the glycerol gradient fractions were assayed for ATPase activity. The ATPase activity profile is shown. The fractions corresponding to the peaks of the internal markers catalase, BSA, and cytochrome c are indicated by vertical arrows.

Interestingly, the comparison of the full deletion and the truncated *cshA* mutant strains revealed a large similarity in the RNA stabilization in respect to the wild type (**Fig. 4A**). From the cumulative distribution of RNA stabilization in the 2 mutant strains it is clear that in both the full deletion and the truncated CshAΔCter mutant strains over 80% of the RNAs are stabilised, but only a relatively small portion is significantly (≥2 fold) stabilised in the absence of the helicase or in absence of the C-terminal extension of CshA (**Fig. 4B**).

To identify genes that had RNAs stabilised at least 2 fold we compared the data of the full deletion and the CshAΔCter mutants with the wild type data. Since the 2 mutant types behaved similarly we retained genes that showed in at least 3 out of the 4 experiments (2 times the full deletion and 2 times the C-terminal truncation) a 2 fold or larger increase of the half-life. We discarded four genes in which one of the half-lives from the wt strain was longer than in one mutant strain. Using these criteria we retained 113 RNAs that were stabilised 2 fold or more (**Table 1**). For many RNAs, the stabilization also leads to an increase of the steady state level, as judged from the number of reads at time zero of the rifampicin treatment (**Fig. 5**).

Similar results were obtained by microarray analysis for RNA preparations carried out at 0, 2.5, 5, 10, and 30 minutes after rifampicin treatment (data not shown). Among 118 identified genes in the micro array experiment, 51 are present in the list obtained by the sequencing approach. The genes that are not present in the final list of the sequencing approach were eliminated due to quality restrictions, low expression levels, or are slightly below the cut-off (≥2×) in the sequencing data set. Nevertheless the overall concordance of the 2 methods validates the sequencing approach. It should be noted that due to our RNA purification, we did not quantitatively purify small RNAs (<200 nt), and we therefore concentrate here on the analysis of coding RNAs. Interestingly, a few mRNAs seemed to be destabilised in absence of a fully functional CshA protein. At present we have no explanation for this.

Altogether these results clearly indicate that CshA is involved at least to some degree in the degradation of many RNAs. Moreover, CshA seems to play a significant role in the turnover of a subset of mRNAs. Moreover, we show that the C-terminal extension of this DEAD-box protein is important for this function within RNA decay.

Identification of CshA interaction partners

The C-terminal truncation of CshA in the CshAΔCter mutant strain showed reduced growth at 16°C but not at higher temperatures. However the analysis of the RNA-decay patterns showed virtually identical profiles for the full deletion and the C-terminal truncation. Thus it is likely that the C-terminal extension is important for interactions with the RNA-decay machinery and we set out to identify interacting proteins using a tandem affinity purification (TAP) approach. We used a PR01Δ*cshA* strain producing a full-length CshA protein or the C-terminal truncated CshAΔCter, containing a Strep/FLAG-tag at the C-terminus. We verified that the tagged version of full length CshA was able to restore the cold sensitive phenotype of the PR01Δ*cshA* strain, showing that the protein is functional (data not shown). We also checked the production of the proteins by western blot, using a polyclonal antibody raised against CshA. We noted a slight overproduction in comparison with the wild type level of CshA, probably due to the fact that the constructs are expressed from a plasmid on its native promoter (data not shown). Since some interactions could be mediated through RNA, we performed the lysis steps both in absence or presence of RNase A. The Strep/FLAG tagged versions of CshA and their potential interaction partners were purified using first a Strep-Tactin column. The corresponding elution fractions were pooled and subjected to a second round of purification on an α-FLAG resin. In order to be able to discriminate protein interactions from column background, we performed in parallel the same purifications with a lysate from a PR01 strain with the empty vector. The eluted fractions were analyzed on a SDS-PAGE and the protein partners were identified by mass spectrometry. A total of 106 proteins were identified in the elution fractions coming from the lysates containing the tagged version of CshA, with or without RNase A treatment (**Table S2, Table S3** for the full data set). Among these proteins, we found proteins involved in each step of the RNA metabolism from transcription to decay, enzymes in DNA metabolism and others. Indeed, we found interactions with the β and β' subunits of the RNA polymerase, various ribosomal proteins, translation initiation and elongation factors. Most importantly, we also identified RNase J1, RNase J2, RNase Y and enolase, components of the putative degradosome. Interestingly, the PNPase was only detected without RNase A treatment, suggesting a lose association, if any, with the degradosome. To identify the interactions mediated through the C-terminal extension, we also identified proteins that copurified with the truncated CshAΔCter. The analysis showed that out of the 106 proteins from the CshA purification, 68 proteins were

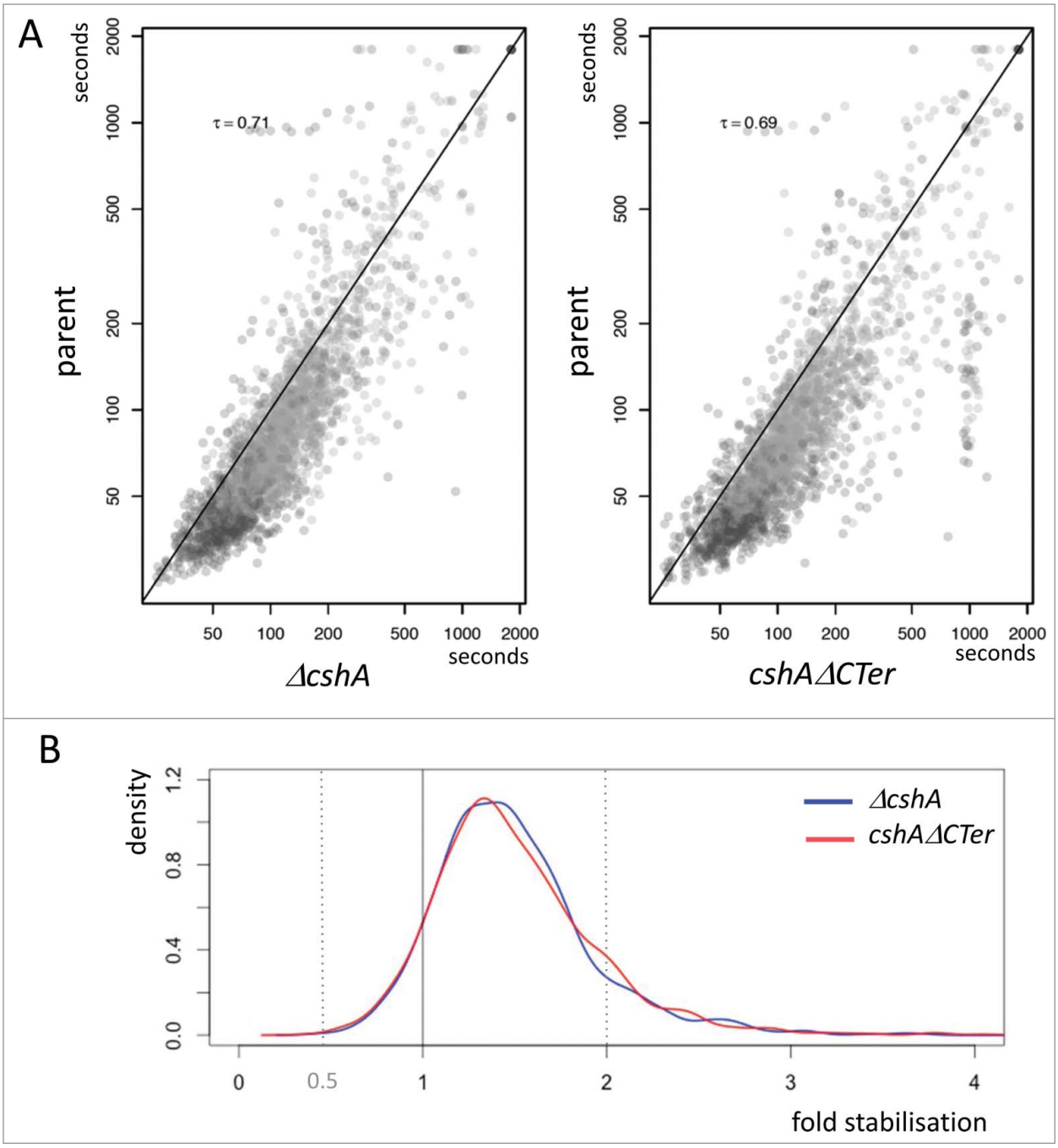

Figure 4. Stabilization of mRNAs. (**A**) Scatterplot showing half-life change between mutants and the parental strain. Each point represents a gene and is positioned on the x-axis according to the mean half-life estimated in both replicates of the decay experiment; similarly, the point on the y-axis is positioned according to the mean half-life estimated in both replicates of the decay experiment of the parental strain. Kendall tau correlation coefficient is given for each case. A diagonal line marks the limit between genes whose half-life is increased in the mutants (below the line), and genes whose half-life is decreased in the mutants (above the line). Only genes satisfying minimum quality criteria are reported. (**B**) Distribution of the half-life fold change between the mutants and the parental strain. The areas under the curves sums to 1.0, and reflects the proportion of genes affected with a given stabilization factor. The vertical line at x = 1 marks the limits between stabilization (on the right) and destabilization (on the left). The shift of the curves on the right side of the vertical line reflects the longer half-life measured in the mutants compared to the ancestor strain.

absent in the CshAΔCter preparation after RNase A treatment (Table 2). Importantly, RNase J1, RNase J2, RNase Y and enolase were no longer detected, as well as many ribosomal proteins, indicating an association mediated through the C-terminal extension. We therefore also purified RNase J1 to see whether the reciprocal co-purification could be observed. Interestingly, relatively few proteins copurified with RNase J1, with the exception of ribosomal proteins and

Table 1. Stabilized RNAs. The half-life of the RNAs in the 2 mutant and the parental strains in 2 independent experiments were compared. The ratio of the half-life of the mutant compared to the parental strain is indicated. Genes that showed a stabilization of the RNA at least 2-fold in 3 out of the 4 mutant strains were retained and are listed in the table

gene ID	operon	Description	Gene Name	First data set		Second data set	
				ΔcshA/wt	CshAΔCter/wt	Δcsha/wt	CshAΔCter/wt
		Stabilized mRNAs					
SA0013	SA0012-SA0016	Cyclic di-AMP phosphodiesterase	GdpP	2.1	2.1	2.2	2.1
SA0014	SA0012-SA0016	Ribosomal protein L9	*rplI*	2.1	2.0	2.0	1.9
SA0127	SA0124-SA0127	Uncharacterized protein, similar to E. coli Putative O-antigen transporter [rfbX]	SA0127	3.4	2.7	2.6	25.8
SA0129		Uncharacterized protein	SA0129	2.9	2.8	3.1	2.4
SA0132	SA0131-SA0134	Uncharacterized protein, weak similarity to Bacillus Tetracycline resistance protein [tetB],	SA0132	2.6	2.4	2.2	2.7
SA0173	SA0173-SA0174	Uncharacterized protein, similar to aminoacid adenylases,	SA0173	3.4	3.1	5.0	3.9
SA0174	SA0173-SA0174	Uncharacterized protein, homolog to Bacitracin synthase 3	SA0174	3.0	3.5	2.6	5.1
SA0198		Oligopeptide transport ATP-binding	*oppF*	1.9	2.0	2.3	3.0
SA0285		Uncharacterized protein	SA0285	2.4	2.1	1.1	3.1
SA0301	SA0300-SA0302	Pseudouridine-5′-phosphate glycosidase	psuG	2.1	1.8	3.1	3.2
SA0309		Lipase 2	*geh*	2.0	2.7	2.3	8.3
SA0318	SA0318-SA0321	Uncharacterized protein, similar to Ascorbate-specific permease IIC component UlaA	*ulaA*	2.1	2.1	2.0	1.8
SA0319	SA0319-SA0321	Uncharacterized protein	SA0319	2.5	2.1	2.2	1.8
SA0430	SA0430-SA0431	Glutamate synthase large subunit	*gltB*	2.7	2.7	3.3	3.7
SA0453	SA0453-SA0456	4-diphosphocytidyl-2-C-methyl-D-erythritol kinase	*ipk*	2.1	2.1	2.3	2.4
SA0454	SA0453-SA0456	purR transcription regulator	*purR*	2.0	2.0	2.1	2.3
SA0475		Lysine-tRNA synthetase	*lysS*	2.4	2.3	2.3	2.1
SA0484	SA0484-SA0485	DNA repair protein radA	*radA*	2.5	2.8	2.7	2.3
SA0485	SA0484-SA0485	Uncharacterized protein, similar to putative Bacillus RNase YacL (PIN and TRAM-domain)	SA0485	2.4	2.9	1.9	3.0
SA0507		Uncharacterized protein, similar to putative amidohydrolase YhaA	SA0507	2.0	2.2	1.9	2.0
SA0578	SA0577 - SA0584	Putative antiporter subunit mnhA2	SA0578	2.3	2.7	1.9	2.1
SA0587	SA0587-SA0589	Uncharacterized protein, similar to Manganese ABC transporter substrate-binding lipoprotein precursor	SA0587	1.8	2.0	2.1	2.3
SA0588	SA0587-SA0589	Uncharacterized protein, similar to Manganese transport system membrane protein MntC	SA0588	1.7	2.0	2.1	2.6
SA0589	SA0587-SA0589	Uncharacterized protein, similar to Manganese transport system ATP-binding protein MntB	SA0589	1.7	2.0	2.4	2.3
SA0682		Uncharacterized protein, similar to Di-/tripeptide transporter [dtpT]	SA0682	2.2	2.1	2.0	1.5
SA0701		Uncharacterized membrane protein with similarity to diguanylate cyclase DgkC	SA0701	3.2	2.9	1.8	3.0
SA0868	SA0863-SA0868	Uncharacterized protein, similar to Putative Na(+)/H (+) antiporter YjbQ [yjbQ]	SA0868	2.5	2.4	1.9	2.2
SA0927	SA0927-SA0929	Uncharacterized protein, weakly similar to Putative HMP/thiamine permease protein YkoC	SA0927	2.3	2.1	1.2	2.0
SA0950	SA0949-SA0954	Spermidine/putrescine import ATP-binding protein	*potA*	2.3	2.3	1.9	2.1
SA0951	SA0949-SA0954	Spermidine/putrescine transport system permease protein	*potB*	2.3	2.5	1.7	2.4
SA0952	SA0949-SA0954	Spermidine/putrescine transport system permease protein	*potC*	2.3	2.4	1.6	4.0
SA0964		Heme A synthase	*ctaA*	2.0	2.1	2.3	1.9
SA0975		Uncharacterized protein	SA0975	2.4	2.0	2.1	1.5
SA0987		Ribonuclease HIII	*rnhC*	2.7	2.7	2.2	2.4
SA1007		Alpha-Hemolysin	hlay	3.6	3.8	2.7	6.4
SA1073	SA1071-SA1074	Malonyl CoA-acyl carrier protein transacylase	*fabD*	2.4	2.2	2.2	2.3
SA1074	SA1071-SA1074	3-oxoacyl-[acyl-carrier-protein] reductase FabG	*fabG*	2.3	2.1	2.1	2.0
SA1139	SA1137-SA1139	Glycerol uptake operon antiterminator regulatory protein	*glpP*	2.2	2.0	1.7	3.0
SA1187		Glycerol-3-phosphate acyltransferase	*plsY*	2.8	2.4	2.8	1.8

(*continued on next page*)

Table 1. Stabilized RNAs. The half-life of the RNAs in the 2 mutant and the parental strains in 2 independent experiments were compared. The ratio of the half-life of the mutant compared to the parental strain is indicated. Genes that showed a stabilization of the RNA at least 2-fold in 3 out of the 4 mutant strains were retained and are listed in the table *(Continued)*

gene ID	operon	Description	Gene Name	First data set		Second data set	
				ΔcshA/wt	CshAΔCter/wt	Δcsha/wt	CshAΔCter/wt
		Stabilized mRNAs					
SA1193		oxacillin resistance-related FmtC protein (fmtC)	*fmtC*	2.4	2.3	1.8	2.4
SA1224		Uncharacterized protein, similar to uncharacterized ABC transporter ATP-binding protein YkpA	SA1224	2.8	2.8	2.0	2.9
SA1267	SA1267-SA1268	Extracellular matrix-binding protein EbhA	*ebhA*	1.6	2.0	7.7	6.1
SA1268	SA1267-SA1268	Extracellular matrix-binding protein EbhB	*ebhB*	2.7	2.6	5.5	5.4
SA1281	SA1279-SA1281	Uncharacterized protein	SA1281	2.7	2.3	2.0	2.8
SA1282	SA1282-SA1283	Holliday junction resolvase RecU	*recU*	3.6	3.0	2.5	2.4
SA1283	SA1282-SA1283	penicillin binding protein 2	*pbp2*	2.6	2.5	2.2	1.5
SA1337		Uncharacterized protein, weakly similar to transcriptional regulator	SA1337	2.3	2.2	1.9	2.0
SA1375	SA1375-SA1380	Uncharacterized protein, similar to Probable metallo-hydrolase YqgX	SA1375	2.0	2.0	2.1	2.1
SA1376	SA1375-SA1380	Uncharacterized protein, Similar to YqgV from B. subtilis	SA1376	2.3	2.2	2.2	2.4
SA1377	SA1375-SA1380	Glucokinase	*glcK*	2.5	2.3	2.8	3.1
SA1474	SA1474-SA1475	Uncharacterized protein	SA1474	2.3	2.0	1.7	2.0
SA1490		Uncharacterized protein	SA1490	2.8	2.7	2.1	6.3
SA1536	SA1535-SA1538	Uncharacterized protein, weakly similar to UPF0721 transmembrane protein	SA1536	2.2	2.2	2.1	2.5
SA1579	SA1578-SA1579	Leucine-tRNA synthetase	*leuS*	1.9	2.0	2.1	2.4
SA1580		Uncharacterized protein, similar to Uncharacterized MFS-type transporter YttB	SA1580	2.3	2.3	2.1	1.9
SA1587	SA1586-SA1589	Riboflavin biosynthesis protein RibA	*ribA*	2.1	1.6	2.1	2.0
SA1588	SA1586-SA1589	Riboflavin synthase α chain	*ribB*	2.1	1.6	2.3	2.0
SA1589	SA1586-SA1589	Riboflavin biosynthesis protein RibD	*ribD*	2.1	1.5	2.4	2.1
SA1606		Uncharacterized protein, similar to Glyoxal reductase	SA1606	2.8	3.6	2.4	3.2
SA1617	SA1617-SA1618	Uncharacterized protein	SA1617	2.8	1.8	3.1	7.0
SA1618	SA1617-SA1618	Uncharacterized protein	SA1618	4.2	2.3	4.1	4.4
SAS053		Uncharacterized protein	SAS053	2.4	2.3	1.1	2.1
SA1679	SA1678-SA1680	Uncharacterized protein	SA1679	2.8	2.6	2.0	3.2
SA1680	SA1679-SA1680	Uncharacterized protein	SA1680	3.1	2.9	1.7	6.4
SA1755		Chemotaxis inhibitory protein, extracellular	SA1755	7.0	2.9	2.0	19.7
SAS066	SA1843-SA1844	AgrD protein	*agrD*	2.7	2.4	3.3	16.8
SA1843	SA1843-SA1844	Accessory gene regulator C	*agrC*	4.2	3.7	2.0	19.3
SA1844	SA1843-SA1844	Accessory gene regulator A	*agrA*	3.3	3.5	2.1	16.9
SA1851		Redox-sensing transcriptional repressor Rex	*rex*	2.3	2.3	2.3	2.0
SA1879	SA1879-SA1881	Potassium-transporting ATPase C chain 1	*kdpC*	3.0	2.9	4.5	6.4
SA1880	SA1879-SA1881	Potassium-transporting ATPase B chain 2	*kdpB*	3.0	2.9	3.8	6.2
SA1881	SA1879-SA1881	Potassium-transporting ATPase A chain 1	*kdpA*	4.0	3.4	2.8	6.5
SA1883	SA1882-SA1883	KDP operon transcriptional regulatory protein KdpE	*kdpE*	2.2	2.3	2.5	2.7
SA1897	SA1893-SA1897	Putative thiaminase-2	SA1897	2.7	2.4	1.1	4.1
SA1923		Transcription termination factor Rho	*rho*	4.1	3.4	3.8	2.6
SA1970		Uncharacterized protein, similar to Uncharacterized MFS-type (major-facilitator-superfamily) transporter YcnB	SA1970	2.1	2.2	2.2	2.2
SA1993	SA1991-SA1997	Lactose-specific phosphotransferase enzyme IIA component	*lacF*	2.3	1.9	2.5	5.4
SA1994	SA1991-SA1997	Tagatose 1,6-diphosphate aldolase	*lacD*	3.4	2.1	2.7	3.3
SA1995	SA1991-SA1997	Tagatose-6-phosphate kinase	*lacC*	2.3	1.6	2.4	3.8
SA1996	SA1991-SA1997	Galactose-6-phosphate isomerase subunit LacB	*lacB*	2.6	1.6	2.3	3.3
SA1997	SA1991-SA1997	Galactose-6-phosphate isomerase subunit LacA	*lacA*	2.5	1.8	2.3	3.9
SA2050		Uncharacterized protein, similar to Guanine/hypoxanthine permease PbuG	SA2050	3.5	3.2	3.3	2.2
SA2069		Cyclic pyranopterin monophosphate synthase accessory protein	*moaC*	2.3	2.7	2.5	2.3
SA2119	SA2119-SA2120		SA2119	2.9	2.5	2.1	3.8

(*continued on next page*)

Table 1. Stabilized RNAs. The half-life of the RNAs in the 2 mutant and the parental strains in 2 independent experiments were compared. The ratio of the half-life of the mutant compared to the parental strain is indicated. Genes that showed a stabilization of the RNA at least 2-fold in 3 out of the 4 mutant strains were retained and are listed in the table *(Continued)*

gene ID	operon	Description	Gene Name	First data set		Second data set	
				ΔcshA/wt	CshAΔCter/wt	Δcsha/wt	CshAΔCter/wt
		Stabilized mRNAs					
		Uncharacterized protein, similar to Uncharacterized oxidoreductase YhxD					
SA2147		TcaR transcription regulator	*tcaR*	2.5	2.4	1.9	17.5
SA2167		PTS system, sucrose-specific IIBC component	*scrA*	3.5	2.5	3.6	2.5
SA2172		Proton/sodium-glutamate symport protein	*gltT*	3.6	3.6	2.9	2.5
SA2174		HTH-type transcriptional regulator SarZ	SarZ	2.5	2.3	1.9	2.6
SA2206		Immunoglobulin-binding protein sbi	*sbi*	2.9	3.3	3.4	6.1
SA2234	SA2234-SA2237	Probable glycine betaine/carnitine/choline ABC transporter opuCD	*opuCD*	1.8	2.0	2.0	2.0
SA2241		Uncharacterized protein	SA2241	2.9	2.7	2.9	2.2
SA2261		Uncharacterized protein, similar to p-aminobenzoyl-glutamate transport protein	SA2261	3.1	4.5	2.0	2.0
SA2327	SA2327-SA2329	pyruvate oxidase	SA2327	4.6	3.9	3.7	4.3
SA2328	SA2327-SA2329	Holin-like protein CidB	*cidB*	4.2	4.2	4.0	4.7
SA2336		ATP-dependent Clp protease ATP-binding subunit ClpL	*clpL*	3.6	2.8	1.3	2.9
SA2354		O-acetyltransferase OatA, cell membrane	SA2354	2.1	2.0	2.1	1.9
SA2361	SA2361-SA2363	Uncharacterized protein	SA2361	2.1	1.8	2.0	2.2
SA2362	SA2361-SA2363	Uncharacterized protein	SA2362	2.2	1.9	2.2	2.2
SA2366	SA2364-SA2367	Uncharacterized protein	SA2366	2.0	2.0	1.4	2.0
SA2368	SA2368-SA2370	Uncharacterized protein	SA2368	2.1	1.9	2.5	2.3
SA2391	SA2390-SA2392	Pantothenate synthetase, pantoate–β-alanine ligase	*panC*	2.3	2.0	1.8	2.0
SA2392	SA2390-SA2392	3-methyl-2-oxobutanoate hydroxymethyltransferase	*panB*	2.4	2.2	2.0	1.7
SA2405		Oxygen-dependent choline dehydrogenase	*betA*	2.0	2.2	2.2	2.0
SA2417	SA2417 -SA2419	Sensor histidine kinase	*BraS*	3.1	2.5	2.9	3.4
SA2418	SA2417-SA2419	transcriptional regulatory protein	*BraR*	4.0	2.7	2.5	3.6
SA2419	SA2417-SA2419	Uncharacterized protein	SA2419	3.5	2.5	3.0	3.1
SA2431		Immunodominant staphylococcal antigen B, extracellular	*isaB*	2.2	2.4	1.8	2.3
SA2440	SA2440-SA2446	Glycosyltransferase stabilizing protein Gtf2, part of part of the accessory SecA2/SecY2 system	*gtf2*	2.1	1.9	2.4	2.8
SA2441	SA2440-SA2446	Glycosyltransferase Gtf1	*gtf1*	2.0	1.9	2.9	2.9
SA2442	SA2440-SA2446	Protein translocase subunit SecA 2	SA2442	2.5	2.1	2.7	2.7
SA2487		Uncharacterized protein, similar to transporter	SA2487	2.1	2.1	2.1	2.1
SA2491		Uncharacterized protein	SA2491	2.4	2.1	1.3	9.4
SA2495		Uncharacterized protein, similar to Cro/Cl family transcriptional regulator	SA2495	2.6	2.5	1.7	2.0
Destabilized mRNAs							
SA0156	SA0144-SA0159	Capsular polysaccharide synthesis enzyme Cap5M	*cap5M*	0.2	0.4	0.4	1.0
SA0194		Uncharacterized protein	SA0194	0.3	0.3	0.5	1
SA1310		Probable L-asparaginase	*ansA*	0.5	0.7	0.5	0.5
SA1532		Putative universal stress protein SA1532	SA1532	0.4	0.5	0.4	0.4
SA1989		Uncharacterized protein similar to Putative NADP-dependent oxidoreductase YfmJ	SA1989	0.2	0.2	0.3	0.4
SA1990		Uncharacterized protein	SA1990	0.3	0.4	0.5	0.6

RNase J2 (**Table S2**). Importantly, purification of RNase J1 allowed the copurification of CshA, further confirming an interaction of CshA and RNase J1. To check for specificity of CshA, we also purified CshB by the same procedure. In contrast to CshA, relatively few proteins copurified with CshB. However, both helicases purified with a considerable number of ribosomal proteins (**Table S2**), which may reflect an association with the ribosome or a role in ribosome biogenesis.[35]

Intriguingly we were so far unable to demonstrate an *in vitro* interaction of individually prepared recombinant N-terminal Flag-Streptavidin tagged RNase J1 with CshA. This could be explained either by cotranslational folding or by interaction through a third partner. However, if both proteins were co-expressed together in *E. coli*, purification of Flag-Streptavidin tagged RNase J1 in presence of RNase A, allowed co-purification of low amounts of CshA, visible on Commassie blue stained gels and confirmed by western blot analysis (data not shown).

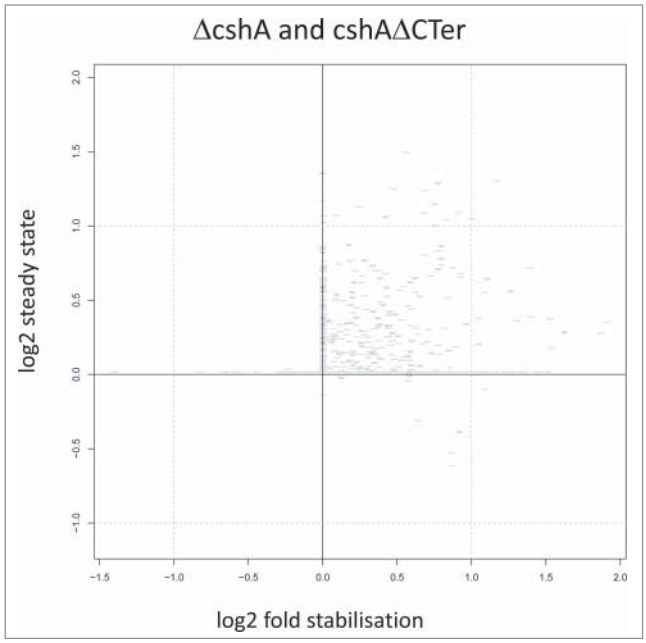

Figure 5. Correlation of half life and steady-state levels. Scatterplot showing correlations between the changes in steady state level of RNAs a time point 0 and in the half-life from the Δ*cshA* and *cshA*Δ*Cter* mutants as compared to the parent. Each point represents a gene and is positioned on the x-axis according to log2 change in half-life (stabilization), while it is positioned on the y-axis according to log2 of the expression of the gene at time point 0 (steady-state level). Each change is computed in a conservative way making use of all replicates information in a worst case scenario strategy: to estimate the change in steady state level, the normalized gene expression of the 2 parent replicates at time point 0 are compared to the normalized gene expression of the 4 mutants at time point 0; only the combination yielding the smallest change is considered. Half-life change on the y-axis is computed with the same strategy.

Interestingly the *H. pylori* RNase J and RNA helicase interaction was also observed only by co-expression.[26]

Discussion

We have previously shown that the *S. aureus* CshA DEAD-box RNA helicase is required for efficient turnover of the *agr* mRNA and that inactivation of *cshA* results in decreased biofilm formation and increased hemolysis. Here we showed that CshA is more generally involved in RNA turnover and that the C-terminal extension is required for this activity, as well as for the interaction with components of a Gram-positive degradosome. Interestingly, the cold sensitive phenotype at 24°C was almost absent with the truncated protein, but very pronounced with the full deletion. We also showed that in absence of the C-terminal extension the RNA-dependent ATPase activity was reduced.

Using the strains PR01Δ*cshA* and PR01*cshA*ΔCter, we were able to show that the bulk of the mRNAs is slightly stabilised in absence of a fully functional CshA protein and that a defined subset of the mRNAs is significantly stabilised in absence of a wild-type helicase. As expected from our previous observations, the *agr* quorum sensing system is among the identified operons. In addition, 2 other 2-component systems, BraS/BraR and Kpd/KpdD) (KpdD was eliminated because of quality limitations) and 6 putative or established transcription factors (purR, SA1337, Rex, tcaR, SA2174, SA2495), as well as genes encoding proteins involved in intracellular signaling, such as the cyclic-di-AMP phosphodiesterase GdpP,[36,37] were among the genes with stabilised mRNAs. Interestingly, many genes encoding membrane-associated proteins (36) were also in the list of significantly stabilised mRNAs. At present we do not know if this observation has a biological significance, or if this is due to a potential localization of the degradosome to the membrane through the RNase Y membrane anchor. The stabilization of RNA could be due to a direct effect of a deficient degradosome, or due to an indirect effect. As an example, studies from the Dunman laboratory have shown that certain mRNAs require SarA for stabilization, which was suggested to be due its RNA binding activity.[34,38] Several RNAs that were identified in the study by[38] are also present in our list of 2 fold or more stabilised RNAs (radA, ctaA, rpmF, glnP fmtC, agrA, kdpA, lacA, moaC, pyruvate oxidase, opuCD, cidB, betA). The *sarA* mRNA is slightly stabilised in the Δ*cshA* strain (1.6-fold) and the *cshA*ΔCter strain (2.2-fold). Moreover, DEAD-box proteins were shown to be able to remove RNA-binding proteins from their substrate,[39] and therefore SarA stabilised mRNAs might be stabilised in absence of CshA either by increased SarA or due to the absence of a putative RNPase activity of the RNA helicase. In a similar vein, certain genes, affected in absence of a fully functional CshA RNA helicase, comprise also genes like the one encoding α hemolysin (SA1007), which is regulated by RNA III. In this case, the stabilization of the mRNA may be due to increased translation upon up-regulation of RNA III as a consequence of the *agr* operon mRNA stabilization (this study and[25]). In accordance with the analysis of CshA in *B. subtilis*,[35] the mRNA encoding the holin-like protein CidB is also largely stabilized in our experimental conditions. Altogether, this suggests that the helicase plays an important role in adaptation to changing environments and thereby influence the outcome of infections by this feared pathogen.

From the studies with the *E. coli* degradosome, it was strongly suggested that the helicase is required for RNAs that contain secondary structures. It is reasonable to expect that mRNAs, coding for proteins that are required only under certain growth conditions or that are involved in adaptation to stress conditions, need to be rapidly turned over when no longer necessary. Therefore one possibility could be that the CshA-dependent decay of RNAs is regulated by the RNA helicase. In this scenario the CshA protein plays a regulatory role, eventually assisted by other proteins. How the helicase itself would be regulated is not known, but in *E. coli*, regulatory proteins that inhibit the RhlB helicase have been described.[8,9] Another more direct explanation for the requirement of a DEAD-box RNA helicase in turnover would be the presence of secondary structures that perform a biological function, such as regulating the accessibility of the ribosome-binding site. For the degradation of such RNAs, the degradosome needs to be assisted by a helicase since it was shown

Table 2. Summary of proteins identified for CshA. Proteins identified in the purifications of CshA, CshAΔCter, RNase J1, or CshB. Numbers represent the peptides identified in presence and absence (within brackets) of RNase A during the purification. The table was established by selecting, for each purification, all proteins that were represented by 2 or more peptides. Proteins were retained for the table if they were present in the CshA purification and after RNase A treatment, but not in the purification of the truncated CshAΔXτερ. The full data set is given in Supplementary Table 3 Proteins identified in the mock sample (Elongation factor Tu, A5IQA2 (14 peptides) and Pyruvate dehydrogenase E1 P0A0A1 (5 peptides)) are not indicated

gene name	Identified Proteins	MW	CshA + (−) RNase	CshAΔCter + (−) RNase	RNase J1 " (−) RNase	CshB + (−) RNase
	RNA METABOLISM					
CshA	CshA (used as bait for the purification in first column)		29 (27)	31 (32)	18 (17)	4 (12)
rnj1	Ribonuclease J 1	63 kDa	11 (13)		56 (54)	
rnj2	Ribonuclease J 2	63 kDa	4 (8)		37 (31)	
rny	Ribonuclease Y	59 kDa	4 (4)			
eno	Enolase	47 kDa	12 (11)			
rpsD	30S ribosomal protein S4	23 kDa	7 (10)	(2)	10 (12)	12 (10)
rpsF	30S ribosomal protein S6	12 kDa	3 (6)		4 (5)	6 (6)
rpsG	30S ribosomal protein S7	18 kDa	4 (5)		4 (8)	7 (7)
rpsL	30S ribosomal protein S9	15 kDa	2 (3)	(2)	4 (4)	4 (4)
rpsL	30S ribosomal protein S12	15 kDa	2 (3)		(2)	
rpsM	30S ribosomal protein S13	14 kDa	4 (5)		3 (5)	4 (4)
rpsR	30S ribosomal protein S18	9 kDa	2 (4)		3 (2)	3 (4)
rpsS	30S ribosomal protein S19	11 kDa	2 (2)			
rplB	50S ribosomal protein L2	30 kDa	12 (13)	(2)	11 (13)	10 (13)
rplC	50S ribosomal protein L3	24 kDa	3 (8)		7 (7)	4 (8)
rplD	50S ribosomal protein L4	22 kDa	6 (7)		3 (5)	5 (5)
rplO	50S ribosomal protein L15	16 kDa	7 (10)	(2)	6 (7)	8 (15)
rplR	50S ribosomal protein L18	13 kDa	2 (2)		2 (3)	4(7)
rplS	50S ribosomal protein L19	13 kDa	4 (4)		6 (5)	5 (7)
rplT	50S ribosomal protein L20	14 kDa	2 (5)		2 (2)	2 (3)
rplU	50S ribosomal protein L21	11 kDa	6 (7)	(3)	6 (5)	8 (8)
rplV	50S ribosomal protein L22	13 kDa	4 (3)	(2)	3 (2)	3 (4)
rplW	50S ribosomal protein L23	11 kDa	2 (5)		2 (3)	2 (5)
rpmC	50S ribosomal protein L29	8 kDa	3 (4)		2	3 (3)
rpmE2	50S ribosomal protein L31	10 kDa	2			3 (4)
rsmA	rRNA small subunit methyltransferase A	34 kDa	3			
infB	Translation initiation factor IF-2	78 kDa	3 (3)			
serS	Serine–tRNA ligase	49 kDa	2			
METABOLISM						
ald1	Alanine dehydrogenase 1, SA1272	40 kDa	3			
adh	Alcohol dehydrogenase	36 kDa	10 (3)			
atpF	ATP synthase subunit	20 kDa	2			
qoxB	Probable quinol oxidase subunit 1	75 kDa	3			
qoxA	Probable quinol oxidase subunit 2	42 kDa	3			
ubiE	Demethylmenaquinone methyltransferase, menaquinone biosynthesis	27 kDa	3			
pyrR	Bifunctional protein PyrR, RNA binding	20 kDa	3	(2)		
ftnA	Ferritin	20 kDa	5 (4)			5 (4)
glmS	Glutamine–fructose-6-phosphate aminotransferase	66 kDa	4			
relA	GTP pyrophosphokinase, ppGpp formation	85 kDa	4 (6)			
pgk	Phosphoglycerate kinase	43 kDa	2			
lacF	Lactose-specific phosphotransferase enzyme IIA component	11 kDa	2			
lacE	PTS system lactose-specific EIICB component	62 kDa	3			
ptsG	PTS system glucose-specific EIICBA component	74 kDa	4			
glcB	PTS system glucoside-specific EIICBA component	74 kDa	6			
murA1	UDP-N-acetylglucosamine 1-carboxyvinyltransferase 1	45 kDa	10			
kdpB	Potassium-transporting ATPase B chain	73 kDa	2			
ugtP	Processive diacylglycerol glucosyltransferase	45 kDa	2			
gtaB	UTP–glucose-1-phosphate uridylyltransferase	32 kDa	4 (3)			
SA0216	Uncharacterized TCS response regulatory protein	30 kDa	2			
saeS	Histidine protein kinase SaeS, TCS	40 kDa	4			
hslU	ATP-dependent protease ATPase subunit HslU, protein degradation	52 kDa	2			
ftsH	ATP-dependent zinc metalloprotease FtsH, protein degradation	81 kDa	3			
OTHER FUNCTIONS						
esaA	Protein EsaA, protein secretion	115 kDa	5			

(*continued on next page*)

Table 2. Summary of proteins identified for CshA. Proteins identified in the purifications of CshA, CshAΔCter, RNase J1, or CshB. Numbers represent the peptides identified in presence and absence (within brackets) of RNase A during the purification. The table was established by selecting, for each purification, all proteins that were represented by 2 or more peptides. Proteins were retained for the table if they were present in the CshA purification and after RNase A treatment, but not in the purification of the truncated CshAΔXτερ. The full data set is given in Supplementary Table 3 Proteins identified in the mock sample (Elongation factor Tu, A5IQA2 (14 peptides) and Pyruvate dehydrogenase E1 P0A0A1 (5 peptides)) are not indicated *(Continued)*

gene name	Identified Proteins	MW	CshA + (−) RNase	CshAΔCter + (−) RNase	RNase J1 " (−) RNase	CshB + (−) RNase
	RNA METABOLISM					
ezrA	Septation ring formation regulator EzrA	66 kDa	14			
map	Protein map, 4 microtubule associated protein motifs	53 kDa	3 (3)		2 (2)	
SA1813	Uncharacterized leukocidin-like protein 2	40 kDa	4 (5)			
uvrA	UvrABC system protein A	105 kDa	2 (8)			
gyrB	DNA gyrase subunit B	73 kDa	2			
ftsK	DNA translocase FtsK	88 kDa	3 (3)			
fmtA	Protein FmtA, unknown function,	46 kDa	3 (5)			
lip2	Lipase 2	76 kDa	2			
clfB	Clumping factor B	97 kDa	4			
spa	Immunoglobulin G-binding protein A	56 kDa	4 (6)			
sbi	Immunoglobulin-binding protein sbi	50 kDa	5			
spsB	Signal peptidase IB	22 kDa	3			
ssaB	Staphylococcal secretory antigen ssaA2	29 kDa	4 (3)			
femX	Lipid II:glycine glycyltransferase	49 kDa	8 (9)			8 (7)
SA0778	UPF0051 protein	53 kDa	2			
SA1727	UPF0316 protein	23 kDa	2			
SA1560	UPF0478 protein	19 kDa	2 (2)			

previously that both the 5′-3′ RNase J and the 3′-5′ PNPase are sensitive to secondary structures.[40,41] However, it remains to be shown, whether CshA is a permanent member of the decay machinery, or if it is only recruited on demand. A detailed analysis of some of the target RNAs requiring CshA will certainly help to further distinguish between these possibilities.

RNA turnover in *S. aureus* has been analyzed previously in exponential phase, heat shock, cold shock, stringent and SOS response conditions.[42] Under heat shock, cold shock and stringent response conditions, the stability of most mRNAs increased, but so far the components required for the turnover have not been identified. Using tandem affinity purifications we were able to determine the interaction partners of CshA, CshAΔCter, RNase J1 and CshB. Importantly, CshA copurifies with the predicted degradosome proteins RNase J1, RNase J2, RNase Y and enolase. This is consistent with bacterial 2-hybrid analyses[23] and the finding that the minimal *H. pylori* degradosome is formed by RNase J and RhpA.[26] In addition we noted that CshA interacts with 28 ribosomal proteins and various other proteins. Most of these interactions are lost when the purification is performed with CshAΔCter, indicating that the C-terminal region drives these interactions. However, it should ne noted that many of these interactions might be indirect. Nevertheless it was shown that both the *H. pylori* and the *E. coli* degradosomes associate with poly-ribosomes[18,26] and that RNase J1 and RNase J2 from *B. subtilis* are tightly ribosome associated. Moreover, most ribosomal proteins that copurified with CshA were also found in the purification of RNase J1. Finally, CshA was reported to be involved in ribosome biogenesis in the same bacterial species.[35] To distinguish between an interaction with RNase J or the ribosome, we intended to co-purify recombinant RNase J1 and CshA. However, so far we were not able to demonstrate co-purification by mixing the purified proteins, but found a weak interaction if co-expressed together in *E. coli* (data not shown). Further experiments will be required to confirm or reject such a putative interaction between CshA and RNase J1, or an indirect interaction through the ribosome. We observed that CshA copurifies with a higher number of proteins than RNase J1 and CshB and that many more proteins unrelated to RNA metabolism co-purify with CshA. It is not clear to what extent CshA could be associated with translating ribosomes or could be anchored to the membrane through its interaction with RNase Y[24,43] and thereby indirectly co-purify with a large number of proteins.

It has been shown for several DEAD-box proteins that N- and C-terminal extensions are important for interactions with either their substrate or partner proteins, and thereby confer specificity to these RNA-dependent ATPases. Here we showed that the deletion of the C-terminal 124 amino acids results in reduced growth at low temperature (16°C) and stabilization of the *agr* mRNA similar to the full deletion. The slightly better growth at 24°C indicates that the truncated helicase, despite reduced enzymatic activity (see below) and the absence of many interacting proteins, retains some functionality which may be provided by interactions through the core domain, as it is observed for the minimal RNA helicases eIF4A or eIF4AIII, interacting with eIF4G and the exon-junction complex components, respectively.[44,45] It may also support the hypothesis that CshA is involved in another process, such as ribosome biogenesis. Indeed, in *E. coli* the deletion of RhlB does not confer a cold sensitive phenotype, whereas the deletion of CsdA/DeaD or SrmB results in cold-sensitivity, probably due to erroneous 23S rRNA•5S

rRNA hybridization, as elegantly shown with a *srmB* suppressor analysis.[46] Such a ribosome biogenesis function was also suggested for the *B. subtilis* CshA[35] and would be in accordance with the co-purification of a large number of ribosomal proteins.

Altogether, our results show that CshA is required for efficient turnover of the bulk of mRNAs and that a selected subset of RNAs is significantly stabilised in absence of the RNA helicase. For efficient degradation, the RNA helicase interacts through its C-terminal extension with the degradosome components. The molecular function of the RNA helicase could be the destabilisation of secondary structures or the removal of hindering RNA binding proteins. Further analysis of individual RNAs and different mutants in *cshA* or the other components of the degradosome will help to further elucidate this exciting and important aspect of gene expression.

Materials and Methods

Bacterial strains

Bacteria (**Table 3**) were grown under standard laboratory conditions. The deletion mutants were constructed using the *pyrFE*/FOA counter selection system.[30] Standard molecular biology methods for plasmid and strain constructions were employed according to either the manufacturer's instructions or Sambrook and Russell.[47] Plasmids used in this study are listed in **Table 4**.

RNA isolation, GeneChip analysis and RNA-sequencing

Overnight cultures were diluted in fresh Mueller-Hinton media to a final OD_{600} of 0.05. Cells were grown until mid-exponential phase (OD 0.3 – 0.4). A 1 ml sample was harvested and rifampicin was immediately added to arrest the transcription (final concentration 200 μg/ml). 1 ml samples were harvested at 0, 2.5, 5, and 10 minutes after rifampicin treatment. After centrifugation, the supernatant was removed and 0.5 ml of ice-cold acetone-ethanol (1:1) was added and the samples were stored at −80°C until the lysis step. For the lysis, the pellet was resuspended in 200 μl of TE containing 0.05 μg/ml lysostaphin and was incubated 10 minutes at 37°C. The RNA isolation was done immediately after, using the QIAshredder and RNeasy mini column, according to the manufacturer's recommendations (Qiagen). 1 ug of total RNA were ribo-depleted using the ribo-zero magnetic kit for Bacteria from epicenter. Libraries were then prepared using the Illumina TruSeq stranded mRNA kit according to manufacturer's recommendations. Libraries were validated on the Bioanalyzer 2100 (Agilent) and the Qubit fluorimeter (Invitrogen). Samples were multiplexed by 8 and loaded at 8 pM on one lane of a Illumina HiSeq 2500 according to a single read – 50 cycles protocol. Alternatively, RNA was then reverse transcribed, and cDNA was fragmented, 3′-biotinylated, mixed with exogenous labeled "spike-in" transcripts, and hybridized to *S. aureus* GeneChips by following the manufacturer's recommendations for antisense prokaryotic arrays (Affymetrix, Santa Clara, CA).

Assembly of the Staphylococcus aureus SA564 genome

Total DNA was sequenced in a HiSeq 2500 machine using Illumina technology to obtain paired 100 nt reads, which were assembled into 13 contigs with the aid of the complete genome sequence from the closely related *S. aureus* N315.[48] One contig was a circular plasmid (pSA564), and the relative order of the remaining 12 contigs was inferred from the *S. aureus* N315 chromosome, whereupon unique primers were designed to PCR-amplify across the gaps. All 12 gap-spanning PCR products could be obtained, thus confirming the contig-order, and the PCR products were sequenced individually by primer-walking with Sanger-sequencing to completely fill the gaps and generate a closed circular assembly. Finally, the original Illumina reads were re-mapped onto the SA564 assembly, and regions of uncertainty were PCR-amplified and confirmed/corrected with Sanger-sequencing. The final assembly was submitted to the NCBI database with accession number CP010890 and CP010891.

Bioinformatic analysis

The stranded mRNA-sequencing reads were mapped to the genome of *S. aureus* N315 using the software BWA.[49] Reads that did align to multiple positions on the genome are dropped. The number of reads overlapping a gene was counted taking into consideration the agreement between the mapped read strand and the gene strand. This was done under the R programming language environment (www.R-project.org), making use of Bioconductor packages (www.bioconductor.org). Obtained counts were normalized according to the count obtained for gene HU, and scaled to reflect the average expression level of HU in the 2 WT samples.

To include an RNA, we defined a threshold of 100 reads on average across the 4 time points to avoid too much noise in correctly estimating the half-life of a gene. The threshold of 100 was chosen arbitrary and roughly corresponds to a 5% error on the half-life estimate for a difference of 1 in the count. As reference we used the *hu* mRNA which was shown to be highly expressed

Table 3. Strains

Strains		Description	Reference
E. coli strains	DH5α	Standard laboratory cloning strain	Invitrogen
S. aureus strains	PR01	SA564 disrupted for 2 restriction systems and deleted *pyrFE*	30
	PR01Δ*cshA*	PR01 with *cshA* deleted	25
	PR01*cshA*ΔCter	PR01 with *cshA* region corresponding to amino acids 386 to 506 deleted	This study
	PR01Δ*cshB*	PR01 with *cshB* deleted	30
	PR01Δ*J1*	PR01 with *RNaseJ1* deleted	30

Table 4. Plasmids

Name	Description	Reference
pEB01	pCN47 with the cat194 cassette from pCN38 replacing the Erm cassette	[25]
pEB07	pEB01 plasmid with *cshA* gene from SA564 and 542 bp upstream	[25]
pCG	pEB01 plasmid for expression of proteins with a C-terminal Strep/Flag tag	This study
pCG*cshA*	pCG vector with *cshA* gene from SA564 and 542 bp upstream	This study
pCG *cshA*ΔCter	pCG vector with *cshA* gene region from SA564 corresponding to CshA aminoacids 1–385 and 542 bp upstream	This study
pCG*J1*	pCG vector with *RNaseJ1* gene from SA564 and 493 bp upstream	This study
pCG*cshB*	pCG vector with *cshB* gene from SA564 and 589 bp upstream	This study

and stable, and has been used previously.[33] A qRT-PCR analysis of 16S rRNA and *hu* mRNA showed very similar stability over a time range of 10 minutes.

Using log2 transformed expression levels, measured at the 4 time points (0, 2.5′, 5′, 10′), a linear model was fitted to estimate the half-life. Indeed, the level of expression e_t at time t, for a gene characterized by a half-life h, and an expression level e_0 at time 0 is expected to be $e_t = e_0(1/2)^{t/h}$. The Log2 transformation of this formula results in a linear expression in t: $log_2(e_t) = log_2(e_0) - i/h$; so that the half-life is given by: $h = -1/a$ where a is the linear coefficient of the model fitted on the log2 transformed expressions. For simplicity, half-life estimates > 30 minutes, or negative half-lives (as stable as HU or more stable in our experimental conditions) were set to 30 minutes.

Model fitting was effectively performed by minimizing a weighted sum of square errors. Since most of the RNAs have a very short half live resulting in background levels at time point 10 minutes or even earlier, weights were set accordingly (256, 64, 16, and 1 fold, for the 0, 2.5, 5, 10 minutes time points). We empirically determined that fitted models resulting in a weighted error sum higher than 20 are not satisfying and this score was therefore used as cut-off for quality control.

Tandem affinity purification

CshA, CshAΔCter, CshB and RNase J1 were cloned in the pCG vector, resulting in the expression of proteins containing a Strep/Flag tag at their C-terminal extremity. PR01Δ*cshA*, PR01Δ*cshB* and PR01Δ*J1* strains replicating respectively the pCG*CshA* or the pCG*CshA*ΔCter vector, the pCG*CshB*, and the pCG*J1* were grown until OD = 1. One liter of bacteria was harvested and resuspended in lysis buffer (Tris 50 mM pH 7.5; $CaCl_2$ 1 mM; Triton 0.1%; DNaseI; lysozyme) and subjected to 3 freeze/thaw cycles. The lysate was cleared by centrifugation and loaded on a Streptactin column (IBA). The elution fractions were then loaded on a α-Flag column (Sigma). The purifications were done according to the manufacturer recommendations and the yield varied between 55 and 158 μg per preparation. Proteins were identified by LC/MS starting with 10 μg of material. Proteins were considered as being present in the sample if at least 2 different exclusive peptides were detected.

Bacterial expression vectors for recombinant CshA and CshAΔCter

The pET22b-CshA plasmids were transformed into *E. coli* Rosetta (DE3). Cultures (500 ml) derived from single transformants were grown at 37°C in LB medium containing 50 μg/ml ampicillin and 30 μg/ml chloramphenicol until the OD_{600} reached 0.6. The cultures were adjusted to 0.2 mM IPTG and 2% (v/v) ethanol and incubation was continued for 20 h at 17°C. Cells were harvested by centrifugation and stored at −80°C. All subsequent procedures were performed at 4°C. Thawed bacteria were resuspended in 25 ml of buffer A (50 mM Tris-HCl, pH 8.0, 500 mM NaCl, 10% glycerol, 1 mM $MgCl_2$) and supplemented with one tablet of protease inhibitor cocktail (Roche). The suspension was adjusted to 0.1 mg/ml lysozyme and incubated on ice for 30 min. Imidazole was added to a final concentration of 5 mM and the lysate was sonicated to reduce viscosity. Insoluble material was removed by centrifugation. The soluble extracts were mixed for 30 min with 1.6 ml of Ni^{2+}-NTA-agarose (Qiagen) that had been equilibrated with buffer A containing 5 mM imidazole. The resins were recovered by centrifugation, resuspended in buffer A with 5 mM imidazole, and poured into columns. The columns were washed with 8 ml aliquots of 10 and 20 mM imidazole in buffer A and then eluted step-wise with 2.5 ml aliquots of buffer A containing 50, 100, 250, and 500 mM imidazole. The elution profiles were monitored by SDS-PAGE. The 250 mM imidazole eluates containing the CshA polypeptides were stored at −80°C. The protein concentrations were determined using the Bio-Rad dye reagent with BSA as the standard.

Glycerol gradient sedimentation

An aliquot (50 μg) of the nickel-agarose preparation of CshA was mixed with catalase (50 μg), bovine serum albumin (50 μg), and cytochrome c (50 μg). The mixture was applied to a 4.8-ml 15–30% glycerol gradient containing 50 mM Tris-HCl (pH 8.0), 0.25 M NaCl, 1 mM EDTA, and 2 mM DTT. The gradient was centrifuged for 20 h at 4°C in a Beckman SW50 rotor at 48,000 rpm. Fractions (0.17 ml) were collected from the bottom of the tube.

Triphosphatase assay

Reaction mixtures (15 μl) containing 50 mM Tris-HCl, pH 7.5, 1 mM DTT, 2 mM $MgCl_2$, 1 mM [γ-^{32}P]ATP, 400 ng/μl rRNA and CshA as specified were incubated for 15 min at 37°C. The reactions were quenched by adding 3.8 μl of 5 M formic acid. An aliquot (2 μl) of the mixture was applied to a polyethyleneimine cellulose TLC plate, which was developed using 0.5 M LiCl, 1 M formic acid. The radiolabeled material was visualized by autoradiography, and ^{32}Pi formation was quantified

by scanning the TLC plate with laser Scanner Typhoon FLA 7000 (General Electric).

Disclosure of Potential Conflicts of Interest

No potential conflicts of interest were disclosed.

Acknowledgments

We are grateful to Vanessa Khemici for continuous discussion and to Eckhard Jankowsky and Patrick Viollier for comments on the manuscript. RNA-sequencing experiments were performed at the iGE3 genomics platform of the University of Geneva (http://www.ige3.unige.ch/genomics-platform.php). MS/MS protein identifications were performed at the proteomics core facility of the Faculty of Medicine (http://www.unige.ch/medecine/proteomique/protocols.html), and we are very grateful for their help and advices.

Funding

This work was supported by grants from the Swiss National Science Foundation (PL), the Novartis Jubiläumsstiftung (CG), the Boninchi Foundation (PL) and by the Canton of Geneva.

Authors' Contributions

CG and PL developed the project. SH performed biochemical analysis of CshA. SL and JP performed the bioinformatics analysis. PR and JP performed the genome assembly and annotation. CG, SH, and PL analyzed the data. CG and PL wrote the paper.

Supplemental Material

Supplemental data for this article can be accessed on the publisher's website.

References

1. Wertheim HF, Vos MC, Ott A, van Belkum A, Voss A, Kluytmans JA, van Keulen PH, Vandenbroucke-Grauls CM, Meester MH, Verbrugh HA. Risk and outcome of nosocomial Staphylococcus aureus bacteraemia in nasal carriers versus non-carriers. Lancet 2004; 364:703-5; PMID:15325835; http://dx.doi.org/10.1016/S0140-6736(04)16897-9
2. Lowy FD. *Staphylococcus aureus* infections. N Engl J Med 1998; 339:520-32; PMID:9709046; http://dx.doi.org/10.1056/NEJM199808203390806
3. Novick RP, Ross HF, Projan SJ, Kornblum J, Kreiswirth B, Moghazeh S. Synthesis of staphylococcal virulence factors is controlled by a regulatory RNA molecule. Embo J 1993; 12:3967-75; PMID:7691599
4. Chambers HF, Deleo FR. Waves of resistance: Staphylococcus aureus in the antibiotic era. Nat Rev Microbiol 2009; 7:629-41; PMID:19680247; http://dx.doi.org/10.1038/nrmicro2200
5. Archer NK, Mazaitis MJ, Costerton JW, Leid JG, Powers ME, Shirtliff ME. Staphylococcus aureus biofilms: properties, regulation, and roles in human disease. Virulence 2011; 2:445-59; PMID:21921685; http://dx.doi.org/10.4161/viru.2.5.17724
6. Linder P, Jankowsky E. From unwinding to clamping – the DEAD box RNA helicase family. Nat Rev Mol Cell Biol 2011; 12:505-16; PMID:21779027; http://dx.doi.org/10.1038/nrm3154
7. Kossen K, Karginov FV, Uhlenbeck OC. The carboxy-terminal domain of the DExDH protein YxiN is sufficient to confer specificity for 23S rRNA. J Mol Biol 2002; 324:625-36; PMID:12460566; http://dx.doi.org/10.1016/S0022-2836(02)01140-3
8. Gorna MW, Pietras Z, Tsai YC, Callaghan AJ, Hernandez H, Robinson CV, Luisi BF. The regulatory protein RraA modulates RNA-binding and helicase activities of the E. coli RNA degradosome. RNA 2010; 16:553-62; PMID:20106955; http://dx.doi.org/10.1261/rna.1858010
9. Pietras Z, Hardwick SW, Swiezewski S, Luisi BF. Potential Regulatory Interactions of Escherichia coli RraA Protein with DEAD-box Helicases. J Biol Chem 2013; 288:31919-29; PMID:24045937; http://dx.doi.org/10.1074/jbc.M113.502146
10. Iost I, Bizebard T, Dreyfus M. Functions of DEAD-box proteins in bacteria: current knowledge and pending questions. Biochim Biophys Acta 2013; 1829:866-77; PMID:23415794; http://dx.doi.org/10.1016/j.bbagrm.2013.01.012
11. Carpousis AJ. The RNA degradosome of Escherichia coli: an mRNA-degrading machine assembled on RNase E. Annu Rev Microbiol 2007; 61:71-87; PMID:17447862; http://dx.doi.org/10.1146/annurev.micro.61.080706.093440
12. Kaberdin VR, Blasi U. Bacterial helicases in post-transcriptional control. Biochim Biophys Acta 2013; 1829:878-83; PMID:23291566[AQ3]
13. Gao J, Lee K, Zhao M, Qiu J, Zhan X, Saxena A, Moore CJ, Cohen SN, Georgiou G. Differential modulation of E. coli mRNA abundance by inhibitory proteins that alter the composition of the degradosome. Mol Microbiol 2006; 61:394-406; PMID:16771842; http://dx.doi.org/10.1111/j.1365-2958.2006.05246.x
14. Ikeda Y, Yagi M, Morita T, Aiba H. Hfq binding at RhlB-recognition region of RNase E is crucial for the rapid degradation of target mRNAs mediated by sRNAs in Escherichia coli. Mol Microbiol 2011; 79:419-32; PMID:21219461; http://dx.doi.org/10.1111/j.1365-2958.2010.07454.x
15. Singh D, Chang SJ, Lin PH, Averina OV, Kaberdin VR, Lin-Chao S. Regulation of ribonuclease E activity by the L4 ribosomal protein of Escherichia coli. Proc Natl Acad Sci U S A 2009; 106:864-9; PMID:19144914; http://dx.doi.org/10.1073/pnas.0810205106
16. Carpousis AJ. The Escherichia coli RNA degradosome: structure, function and relationship in other ribonucleolytic multienzyme complexes. Biochem Soc Trans 2002; 30:150-55; PMID:12035760; http://dx.doi.org/10.1042/BST0300150
17. Regonesi ME, Del Favero M, Basilico F, Briani F, Benazzi L, Tortora P, Mauri P, Deho G. Analysis of the Escherichia coli RNA degradosome composition by a proteomic approach. Biochimie 2006; 88:151-61; PMID:16139413; http://dx.doi.org/10.1016/j.biochi.2005.07.012
18. Tsai YC, Du D, Dominguez-Malfavon L, Dimastrogiovanni D, Cross J, Callaghan AJ, Garcia-Mena J, Luisi BF. Recognition of the 70S ribosome and polysome by the RNA degradosome in Escherichia coli. Nucleic Acids Res 2012; 40:10417-31; PMID:22923520; http://dx.doi.org/10.1093/nar/gks739
19. Rochat T, Bouloc P, Repoila F. Gene expression control by selective RNA processing and stabilization in bacteria. FEMS Microbiol Lett 2013; 344:104-13; PMID:23617839; http://dx.doi.org/10.1111/1574-6968.12162
20. Khemici V, Poljak L, Toesca I, Carpousis AJ. Evidence in vivo that the DEAD-box RNA helicase RhlB facilitates the degradation of ribosome-free mRNA by RNase E. Proc Natl Acad Sci U S A 2005; 102:6913-8; PMID:15867149; http://dx.doi.org/10.1073/pnas.0501129102
21. Py B, Higgins CF, Krisch HM, Carpousis AJ. A DEAD-box RNA helicase in the *Escherichia coli* RNA degradosome. Nature 1996; 381:169-72; PMID:8610017; http://dx.doi.org/10.1038/381169a0
22. Vanzo NF, Li, YS, Py B, Blum E, Higgins CF, Raynal LC, Krisch HM, Carpousis AJ. Ribonuclease E organizes the protein interactions in the Escherichia coli RNA degradosome. Genes Dev 1998; 12:2770-81; PMID:9732274; http://dx.doi.org/10.1101/gad.12.17.2770
23. Roux CM, Demuth JP, Dunman PM. Characterization of components of the *Staphylococcus aureus* messenger RNA degradosome holoenzyme-like complex. J Bacteriol 2011; 193:5520-6; PMID:21764917
24. Lehnik-Habrink M, Pfortner H, Rempeters L, Pietack N, Herzberg C, Stulke J. The RNA degradosome in Bacillus subtilis: identification of CshA as the major RNA helicase in the multiprotein complex. Mol Microbiol 2010; 77:958-71
25. Oun S, Redder P, Didier JP, Francois P, Corvaglia AR, Buttazzoni E, Giraud C, Girard M, Schrenzel J, Linder P. The CshA DEAD-box RNA helicase is important for quorum sensing control in Staphylococcus aureus. RNA Biol 2013; 10:157-65; PMID:23229022; http://dx.doi.org/10.4161/rna.22899
26. Redko Y, Aubert S, Stachowicz A, Lenormand P, Namane A, Darfeuille F, Thibonnier M, De Reuse H. A minimal bacterial RNase J-based degradosome is associated with translating ribosomes. Nucleic Acids Res 2013; 41:288-301; PMID:23093592; http://dx.doi.org/10.1093/nar/gks945
27. Deikus G, Condon C, Bechhofer DH. Role of Bacillus subtilis RNase J1 endonuclease and 5′-exonuclease activities in trp leader RNA turnover. J Biol Chem 2008; 283:17158-67; PMID:18445592; http://dx.doi.org/10.1074/jbc.M801461200
28. Rogers GW, Komar AA, Merrick WC. eIF4A: The godfather of the DEAD-box helicases. Progr Nucl Acids Res 2002; 72:307-31; http://dx.doi.org/10.1016/S0079-6603(02)72073-4
29. Linding R, Russell RB, Neduva V, Gibson TJ. GlobPlot: exploring protein sequences for globularity and disorder. Nucleic Acids Res 2003; 31:3701-8; PMID:12824398; http://dx.doi.org/10.1093/nar/gkg519
30. Redder P, Linder P. New range of vectors with a stringent 5-fluoroorotic acid-based counterselection system for generating mutants by allelic replacement in staphylococcus aureus. Appl Environ Microbiol 2012b; 78:3846-54; http://dx.doi.org/10.1128/AEM.00202-12
31. Somerville GA, Beres SB, Fitzgerald JR, DeLeo FR, Cole RL, Hoff JS, Musser JM. In vitro serial passage of

Staphylococcus aureus: changes in physiology, virulence factor production, and agr nucleotide sequence. J Bacteriol 2002; 184:1430-7; PMID:11844774; http://dx.doi.org/10.1128/JB.184.5.1430-1437.2002
32. Rozen F, Pelletier J, Trachsel H, Sonenberg N. A lysine substitution in the ATP-binding site of eucaryotic initiation factor 4A abrogates nucleotide-binding activity. Mol Cell Biol 1989; 9:4061-3; PMID:2506440
33. Redder P, Linder P. DEAD-box RNA helicases in Gram-positive RNA-decay. In Methods In Enzymology, E. Jankowsky, ed., 2012a:pp. 369-83
34. Roberts C, Anderson KL, Murphy E, Projan SJ, Mounts W, Hurlburt B, Smeltzer M, Overbeek R, Disz T, Dunman PM. Characterizing the effect of the Staphylococcus aureus virulence factor regulator, SarA, on log-phase mRNA half-lives. J Bacteriol 2006; 188:2593-603; PMID:16547047; http://dx.doi.org/10.1128/JB.188.7.2593-2603.2006
35. Lehnik-Habrink M, Rempeters L, Kovacs AT, Wrede C, Baierlein C, Krebber H, Kuipers OP, Stulke J. DEAD-Box RNA helicases in Bacillus subtilis have multiple functions and act independently from each other. J Bacteriol 2013; 195:534-44; PMID:23175651; http://dx.doi.org/10.1128/JB.01475-12
36. Corrigan RM, Abbott JC, Burhenne H, Kaever V, Grundling A. c-di-AMP is a new second messenger in Staphylococcus aureus with a role in controlling cell size and envelope stress. PLoS Pathog 2011; 7, e1002217; PMID:21909268; http://dx.doi.org/10.1371/journal.ppat.1002217
37. Griffiths JM, O'Neill AJ. Loss of function of the gdpP protein leads to joint beta-lactam/glycopeptide tolerance in Staphylococcus aureus. Antimicrob Agents Chemother 2012; 56:579-81; PMID:21986827; http://dx.doi.org/10.1128/AAC.05148-11
38. Morrison JM, Anderson KL, Beenken KE, Smeltzer MS, Dunman PM. The staphylococcal accessory regulator, SarA, is an RNA-binding protein that modulates the mRNA turnover properties of late-exponential and stationary phase Staphylococcus aureus cells. Front Cell Infect Microbiol 2012; 2:26; PMID:22919618; http://dx.doi.org/10.3389/fcimb.2012.00026
39. Fairman M, Maroney PA, Wang W, Bowers H, Gollnick P, Nilsen TW, Jankowsky E. Protein displacement by DExH/D RNA helicases without duplex unwinding. Science 2004; 304:730-4; PMID:15118161; http://dx.doi.org/10.1126/science.1095596
40. Causton H, Py B, McLaren RS, Higgins CF. mRNA degradation in Escherichia coli: a novel factor which impedes the exoribonucleolytic activity of PNPase at stem-loop structures. Mol Microbiol 1994; 14:731-41; PMID:7534370; http://dx.doi.org/10.1111/j.1365-2958.1994.tb01310.x
41. Laalami S, Zig L, Putzer H. Initiation of mRNA decay in bacteria. Cell Mol Life Sci 2014; 71:1799-828; PMID:24064983; http://dx.doi.org/10.1007/s00018-013-1472-4
42. Anderson KL, Roberts C, Disz T, Vonstein V, Hwang K, Overbeek R, Olson PD, Projan SJ, Dunman PM. Characterization of the Staphylococcus aureus heat shock, cold shock, stringent, and SOS responses and their effects on log-phase mRNA turnover. J Bacteriol 2006; 188:6739-56; PMID:16980476; http://dx.doi.org/10.1128/JB.00609-06
43. Shahbabian K, Jamalli A, Zig L, Putzer H. RNase Y, a novel endoribonuclease, initiates riboswitch turnover in Bacillus subtilis. EMBO J 2009; 28:3523-33; PMID:19779461; http://dx.doi.org/10.1038/emboj.2009.283
44. Andersen CB, Ballut L, Johansen JS, Chamieh H, Nielsen KH, Oliveira CL, Pedersen JS, Seraphin B, Le Hir H, Andersen GR. Structure of the exon junction core complex with a trapped DEAD-box ATPase bound to RNA. Science 2006; 313:1968-72; PMID:16931718; http://dx.doi.org/10.1126/science.1131981
45. Korneeva NL, First EA, Benoit CA, Rhoads RE. Interaction between the NH2-terminal domain of eIF4A and the central domain of eIF4G modulates RNA-stimulated ATPase activity. J Biol Chem 2005; 280:1872-81; PMID:15528191; http://dx.doi.org/10.1074/jbc.M406168200
46. Proux F, Dreyfus M, Iost I. Identification of the sites of action of SrmB, a DEAD-box RNA helicase involved in Escherichia coli ribosome assembly. Mol Microbiol 2011; 82:300-11; PMID:21859437; http://dx.doi.org/10.1111/j.1365-2958.2011.07779.x
47. Sambrook J, Russell DR. Molecular Cloning: A Laboratory Manual, 3rd edn, Cold Spring Harbor, N. Y.: Cold Spring Harbor Laboratory Press, 2001
48. Kuroda M, Ohta T, Uchiyama I, Baba T, Yuzawa H, Kobayashi I, Cui L, Oguchi A, Aoki K, Nagai Y, et al. Whole genome sequencing of meticillin-resistant Staphylococcus aureus. Lancet 2001; 357:1225-40; PMID:11418146
49. Li H, Durbin R. Fast and accurate short read alignment with Burrows-Wheeler transform. Bioinformatics 2009; 25:1754-60; PMID:19451168; http://dx.doi.org/10.1093/bioinformatics/btp324